applied sciences

MDPI

Article

Intraoperative PRO Score Assessment of Actinic Keratosis with FCF Fast Green-Enhanced Ex Vivo Confocal Microscopy

Daniela Hartmann [1,†], Lisa Buttgereit [1,†], Lara Stärr [1], Elke Christina Sattler [1], Lars Einar French [1,2] and Maximilian Deußing [1,*]

[1] Department of Dermatology and Allergy, LMU University Hospital, LMU Munich, 80337 Munich, Germany; daniela.hartmann@med.uni-muenchen.de (D.H.); elke.sattler@med.uni-muenchen.de (E.C.S.)
[2] Department of Dermatology & Cutaneous Surgery, Miller School of Medicine, University of Miami, Miami, FL 33136, USA
* Correspondence: maximilian.deussing@med.uni-muenchen.de; Tel.: +49-89-4400-56010
† These authors contributed equally to this work.

Abstract: Actinic keratoses (AKs) represent a common skin cancer in situ associated with chronic sun exposure. Early diagnosis and management of AKs are crucial to prevent their progression to invasive squamous cell carcinoma. Therefore, we investigated AK PRO score assessment using ex vivo confocal laser microscopy (EVCM) coupled with a novel fluorescent dye, FCF Fast Green, to explore its potential for the precise imaging and discrimination of collagen fibers. AK PRO assessment using EVCM demonstrated excellent conformity (95.8%) with histopathologic examination. The additional utilization of FCF Fast Green dye had no impact on AK visualization but showed a high affinity for collagen fibers enabling clear differentiation of collagen alterations between healthy and sun-damaged skin. The enhanced visualization of collagen fiber changes may aid clinicians in accurately identifying AKs and differentiating them from benign skin lesions.

Keywords: dermatology; non-invasive imaging; reflectance confocal microscopy; skin cancer; bedside histology; actinic keratoses; fluorescent dye; collagen imaging

Citation: Hartmann, D.; Buttgereit, L.; Stärr, L.; Sattler, E.C.; French, L.E.; Deußing, M. Intraoperative PRO Score Assessment of Actinic Keratosis with FCF Fast Green-Enhanced Ex Vivo Confocal Microscopy. *Appl. Sci.* **2024**, *14*, 1150. https://doi.org/10.3390/app14031150

Academic Editors: Athanasios Koutras, Ioanna Christoyianni, George Apostolopoulos and Dermatas Evangelos

Received: 28 December 2023
Revised: 24 January 2024
Accepted: 26 January 2024
Published: 30 January 2024

1. Introduction

Actinic keratoses (AKs) are common precancerous cutaneous lesions that emerge as a result of prolonged exposure to sun, primarily affecting individuals with fair skin and a history of ultraviolet radiation exposure [1,2]. These lesions represent a significant clinical challenge due to their potential to progress into invasive squamous cell carcinoma, necessitating accurate and early diagnosis for effective management [3,4].

In addition to clinical examination, multiple controversial clinical scoring systems have been developed to classify the severity of actinic keratoses [5]. While Cockerell et al. proposed to categorize AKs as keratinocytic intraepithelial neoplasia (KIN) [6], with regard to related types of intraepithelial neoplasia, like vulvar intraepithelial neoplasia (VIN) [7] or anal intraepithelial neoplasia (AIN) [8], Röwert-Huber et al. suggested a purely histologically based classification. According to this graduation, AKs were subdivided into three severity grades (AK I–III) based on the occurrence of atypical keratinocytes across different layers of the epidermis [9]. While, in AK I, atypical keratinocytes are seen in the lower third of the epidermis, AK II shows atypia in the lower two thirds, and AK III throughout the entire epidermis, respectively. Accordingly, this graduation led to the concept of a continuous disease spectrum, implying that AKs proceed from grade I to grade II and III, eventually leading to the formation of invasive growth. Recent research, however, has found that the most common kind of AKs linked with invasive squamous cell carcinoma (SCC) is grade I, which is characterized by atypical keratinocytes predominantly in the basal and suprabasal layers of the epidermis. [10]. As a result, this categorization failed to deliver a reliable risk assessment.

To develop this area of research, and considering the fact that the interaction between the epidermis and dermis, including tumor invasiveness, arises at the dermoepidermal junction zone [11], a histomorphological classification of atypical keratinocytes based on the "basal growth pattern", called (PRO I-III), has been proposed [12].

The PRO score is a frequently used clinical scoring system for AK-based histology findings at the DEJ [13]. While an early-stage PRO I can be recognized by "clustered and atypical keratinocytes in the basal epidermal layers", PRO II reveals "small hemispherical buds from the basal epidermis emerge into the upper papillary dermis". In PRO III, "spiky or filiform papillary elongations of atypical keratinocytes extend into the upper dermis" [13,14].

While visual grading systems often show a high interobserver variability, a study conducted by Schmitz et al., including 21 dermatologists and pathologists, demonstrated a robust inter-rater reliability of AK PRO assessment [12].

Nevertheless, all these classifications are based on histological examinations, which can be costly and time-consuming and may delay a proper treatment initiation. In response, new imaging techniques have gained momentum in recent years, aiming to provide faster and enhanced diagnostic accuracy [15].

Ex vivo confocal laser microscopy (EVCM) has emerged as a powerful diagnostic method offering near-real-time and rapid imaging of freshly excised tissue at cellular and subcellular level. By employing near-infrared lasers and detecting reflected light along fluorescence signals, EVCM provides high-resolution vertical images nearly similar to conventional histopathology [16].

While this technique has already demonstrated its utility in various dermatological applications, including the intraoperative assessment of excision margins as an adjunctive method to Mohs microscopic surgery [17,18], the assessment of melanocytic lesions [19,20], inflammatory skin disorders [21], and superficial skin cancers [17–20,22–25], the evaluation of PRO score assessment in actinic keratoses has not yet been investigated.

To further enhance the specificity and sensitivity of reflectance microscopy, numerous fluorescent dyes with specific binding properties have been developed [17–20,24,26,27]. Among these, FCF Fast Green (FG)—a synthetic substance originally used for coloring food items—has shown its capability in the precise visualization of collagen and elastic fibers.

FCF Fast Green fluorescent dye emits a fluorescent signal in the far-red range at 638 nm, while also being able to be combined with other antibody-coupled labels and/or nuclear stains that also emit signals at shorter wavelengths. When applied and kept in anhydrous conditions, FG is highly selective to collagen. Remarkably, when applied in watery conditions, the specificity of FG binding to collagen is significantly decreased, and elastic fibers are dyed as well. This finding not only emphasizes the need for adequate sample dehydration for generating collagen-specific FG staining; it also expands the scope of the technique for differentiating collagen from elastic fibers [28–30]. While present research has focused on the "in vitro" application of FCF Fast Green in histology and light-sheet microscopy, its use for the EVCM bedside histology of freshly excised tissue has not been reported.

In light of the current diagnostic challenges and the evolving landscape of non-invasive imaging techniques, our study therefore aimed to investigate the feasibility and diagnostic potential of EVCM in AK PRO score assessment coupled with a new staining protocol including FCF Fast Green for discerning collagen alterations in sun-damaged skin, particularly within AK lesions. By comparing the imaging results between AK lesions and healthy, non-sun-exposed skin, we endeavored to elucidate the capacity of FCF Fast Green-enhanced EVCM to aid in the accurate diagnosis of AKs and potentially ameliorate the approach to early detection and management of these precancerous lesions.

2. Materials and Methods

Study Participants: Participants were recruited at the Department of Dermatology and Allergy of the University Hospital at Ludwig Maximilian University (LMU) in Munich

between March and September 2023. Patients included in our study had skin types varying from Fitzpatrick type I to III. Each patient gave written informed consent before inclusion in the study, which was approved by the local ethics committee of the LMU university hospital (Ref.-Nr. 19-150).

Patients with clinically suspected actinic keratoses (AKs) underwent standard biopsy procedures, resulting in 61 samples. Within this number, 13 cases eventually proved to be Bowens disease, invasive squamous cell carcinoma, or basal cell carcinoma in histology and EVCM. To maintain the focus on actinic keratoses, these lesions were excluded from our study, ensuring that only cases with histologically confirmed AK (=48 lesions) were included. The locations of the lesions were mainly on the capillitium, face, and forearms. A total of 32 healthy control skin samples with no history of chronic sun exposure were collected from wound closures and Burow triangles. Sample sizes ranged from 2 to 10 mm.

Ex vivo confocal laser scanning microscopy (EVCM): Prior to imaging, one cohort of the skin samples (25 AK lesions and 17 healthy skin samples) underwent a new staining protocol consisting of incubation in ethanol (0.7 mmol/L), acridine orange (AO) (0.04 mmol/L, Sigma-Aldrich, St. Louis, MO, USA), FCF Fast Green (0.067 mmol/L, Sigma-Aldrich, St. Louis, MO, USA), and NaCl (0.09 mmol/L) for 30 s each. Due to the incubation in ethanol, a sample dehydration with optimal binding of FCF Fast Green to collagen fibers was achieved.

The other cohort (23 AK lesions and 15 healthy skin samples) underwent a previously established staining protocol using acridine orange (0.1 mmol/L, Sigma-Aldrich, St. Louis, MO, USA) followed by phosphate-buffered saline (0.1 mmol/L, Dulbecco's Phosphate Buffered Saline; PBS; pH 7.4) and citric acid (0.1 mmol/L) for so-called aceto-whitening for 30 s each [20]. All samples were fully immersed in the staining solutions, which covered the entire cut surface.

Ex vivo confocal laser scanning microscopy (EVCM) imaging was performed using the Vivascope 2500 G-4 device (Vivascope, Munich, Germany) with two laser wavelengths at 488 nm (blue) and 638 nm (red). Therefore, the tissue probes were placed on object slides (R. Langenbrinck, Emmendingen, Germany), mounted with sponges as well as magnets, and sectioned in vertical mode to reveal all skin layers according to standard histological procedures [31,32].

While the blue 488 nm laser excites acridine orange-stained structures, generating a fluorescence image, the reflection of the red 638 laser usually produces a reflectance image. With the use of the new FCF Fast Green dye, which fluoresces at 638 nm, the red laser can be used either in reflectance mode (with the pinhole filter open) or in fluorescence mode with FCF Fast Green staining (pinhole filter activated) (Figure 1a). Analogously to previous studies, both of these fluorescence images can be merged together to produce a digital HE (dHE) image similar to a traditional histopathological examination (Figure 1b–d) [24].

Histological analysis and correlation:

After imaging, the skin samples from both cohorts were immediately fixed in 4% buffered formalin and subsequently processed for routine paraffin embedding. A histological analysis was conducted on paraffin-embedded skin sections stained with hematoxylin and eosin (H&E). A histological assessment of PRO score was performed by an experienced dermatopathologist blinded to the clinical and imaging data.

EVCM image analysis:

All images were analyzed by two experienced examiners (L.B., M.D.), who were blinded to the clinical diagnosis and staining protocol. To mitigate biases, the examiners reviewed both AO and FCF images for all cases in a randomized order. Nevertheless, good interobserver agreement was found for all parameters. Disagreements were resolved by the involvement of a third senior dermatologist (D.H.). The following EVCM features were analyzed:

1. Actinic keratosis assessment: Referring to Schmitz et al. [12], we calculated the PRO score to grade the severity of AKs in the EVCM images. The PRO score is a semi-quantitative scoring system that assigns a numerical value to the basal proliferation

and protrusions of the AK lesion at the level of the DEJ. PRO I is accompanied by a close crowding of atypical keratinocytes, while PRO II shows small buds and prominent round nests of atypical keratinocytes starting to protrude into the upper papillary dermis. PRO III is characterized by the spiky or filiform papillary elongation, the so-called papillary sprouting, of atypical keratinocytes protruding into upper dermal structures—still without signs of invasion.

2. Morphological features of solar elastosis: The FCF fluorescence images obtained from the new staining protocol were compared with the reflectance images gained from the standard protocol. The examiners were asked to visually grade collagen fiber alterations as predefined patterns called "regular fibers" or "blurred lines", or as "degeneration" [33]. Descriptive statistics were calculated to summarize the key morphological features. For statistical analysis, continuous variables were described by mean, standard deviation, and 95% confidence interval. A p-value less than 0.05 was considered statistically significant.
3. For the quantification of collagen fiber imaging, we evaluated the brightness intensity using the ImageJ software (Wayne Rasband and contributors, National Institutes of Health, USA, Version 1.53t). Therefore, for each individual image we measured the mean pixel intensity of collagen fibers at three representative locations. To adjust for differences in laser energy or dye concentration, we then calculated the mean pixel intensity of three representative keratinocyte nuclei, which showed no binding affinity to FCF as a reference point, and divided both values to obtain a fiber brightness index (=FBI). If, due to the progression of elastosis, there were no fibers clearly identifiable, the brightness of the degeneration pattern was assessed (exemplary see Figure 2). To reduce any overlap with background signals, a 6 × 6-pixel region of interest was applied, respectively. When keratinocyte nuclei were selected as reference points, they mostly exhibited the same brightness throughout the image, so there was not a large selection to be made.

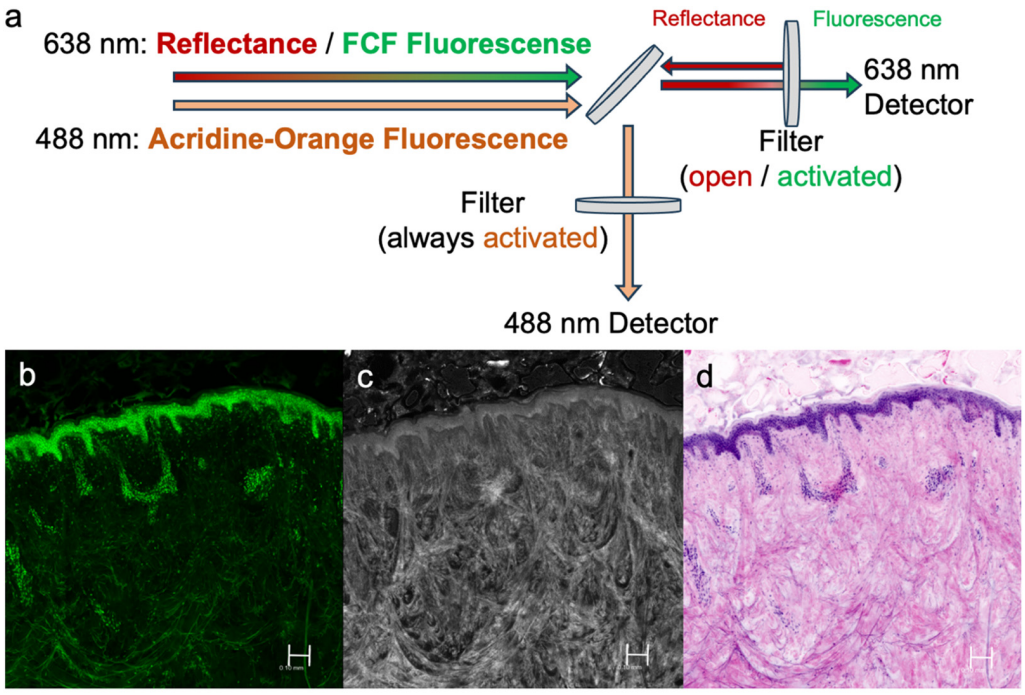

Figure 1. Functionality of EVCM: 638 nm laser can either be utilized in reflection mode (filter open) or in FCF Fast Green fluorescence mode (filter activated). The 488 nm laser is equipped with a permanently active filter utilizing acridine orange (AO) for fluorescence (**a**). Healthy, non-sun-exposed skin scanned with the EVCM device (Vivascope 2500M-G4) in AO fluorescence mode (**b**), FCF fluorescence mode (**c**), and digital HE mode (**d**).

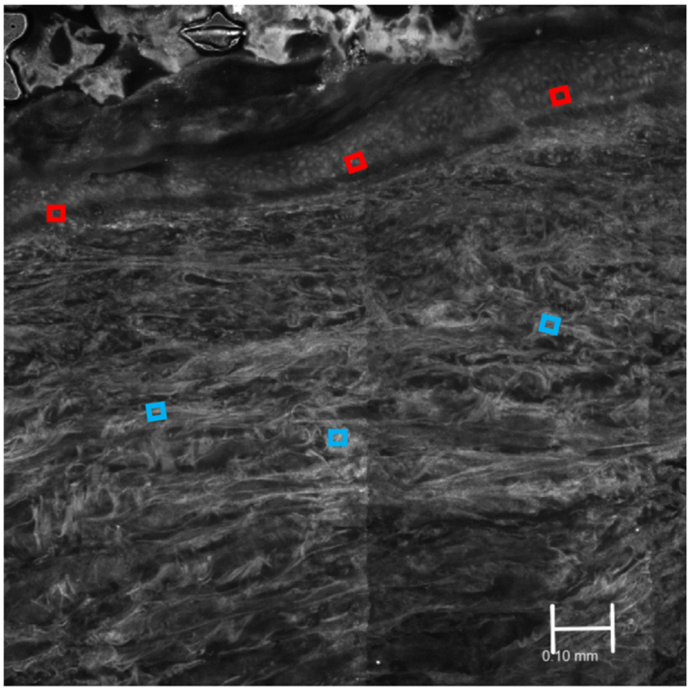

Figure 2. Calculation of the fiber brightness index (=FBI). FCF fluorescence image showing exemplarily the selection of representative collagen fibers (blue squares) and three basal keratinocytes as reference (red squares).

3. Results

The study included 48 participants with histologically confirmed actinic keratoses (AKs) and 32 healthy control participants. The mean age of participants in the AK group was 78.5 years, with a male-to-female ratio of 30 males to 18 females. In the healthy control group, the mean age was 53 years, with a male-to-female ratio of 15 males and 17 females. All AK lesions were located in sun-exposed areas, predominantly on the face, scalp, dorsal hands, and forearms. Healthy control skin samples were reported with no history of chronic sun exposure.

3.1. EVCM PRO Score Assessment of AK Lesions

EVCM imaging successfully captured detailed morphological features of AK lesions: with FCF-EVCM imaging, we saw densely packed atypical keratinocytes near the basement membrane in six lesions, categorizing them as PRO I (Figure 3a). Prominent round nests of atypical keratinocytes starting to protrude into the upper papillary dermis were visible in eleven lesions, grading them as PRO II (Figure 3b). Eight lesions showed remarkable papillary sprouting and elongation of atypical keratinocytes protruding into upper dermal structures, grading them as PRO III (Figure 3c). Using the classical acridine orange-only staining protocol without FCF, six lesions were identified as PRO I, eight lesions as PRO II, and nine lesions as PRO III.

3.2. PRO Score Histological Correlation

The comparison of EVCM PRO score assessment with gold-standard histology demonstrated a strong concordance for both assessment methods, with an overall diagnostic agreement of 46/48 lesions (95.8%). Divided into both cohorts using FCF Fast Green staining, 24/25 lesions (96%) were correctly graded (6/6 of PRO I, 11/12 of PRO II, and 7/7 of PRO III). For classical acridine orange staining, 22/23 lesions (95.6%) were classified correctly (6/6 of PRO I, 8/9 of PRO II, and 8/8 of PRO III). The two EVCM cases that did not agree with histology were both overclassified as PRO III in EVCM, while histological assessment reported PRO II (see Table 1).

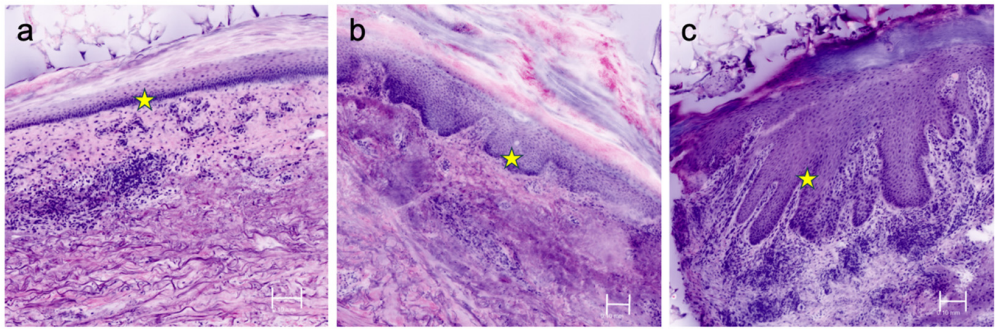

Figure 3. PRO score assessment of actinic keratosis using digital HE–EVCM. The yellow star shows dermoepidermal junction site (DEJ) with intensified basophilic appearance of the crowding keratinocytes in PRO I (**a**), budding of the keratinocytes in PRO II (**b**), and prolonged undulations protruding into the upper dermis in PRO III (**c**).

Table 1. Confusion tables showing lesion-wise PRO score histological correlation for each staining protocol.

		EVCM FCF Fast Green		
		PRO I	PRO II	PRO III
histology	PRO I	6	0	0
	PRO II	0	11	1
	PRO III	0	0	7
		EVCM Acridine Orange		
		PRO I	PRO II	PRO III
histology	PRO I	6	0	0
	PRO II	0	8	1
	PRO III	0	0	8

Importantly, FCF staining had no discernible impact on PRO score assessment compared to the standard AO staining, as evidenced by nearly similar agreement rates with histology.

3.3. EVCM Imaging of Collagen Fibers

Regarding the progress of solar elastosis, we saw three different patterns of alterations in collagen microarchitecture. In sun-damaged skin, regular architecture was seen in 6/48 of the cases (Figure 4a,d). Alterations with incipient degradation, visible as "blurred lines", were perceived in 28/48 lesions (Figure 4b,e), while total destruction, resulting in a "degeneration" pattern, was visible in 28/48 cases (Figure 4c,f). Concerning healthy skin tissue, the "blurred line" pattern was visible in 4/17 lesions for FCF Fast Green and 1/15 for acridine orange staining. "Degeneration" pattern was not depictable. Comparing both staining methods, the new FCF Fast Green-enhanced imaging allowed for better visualization of collagen fibers within the skin, facilitating their clear demarcation in AK lesions and control skin.

3.4. Quantitative Assessment

For the quantitative assessment of collagen imaging, the fiber brightness indexes (FBI) were calculated. We saw remarkably significant differences between AK lesions and control skin for both staining protocols. Regarding AK lesions, FCF staining exhibited a clearly higher FBI compared to regular acridine orange staining (1.89 vs. 1.00; $p < 0.001$). Calculating the FBI in healthy, non-sun-exposed control skin, we saw similar proportions, with an FBI of 1.98 for FCF and 1.24 for regular acridine orange staining ($p < 0.001$) (see Figure 5). These findings align with our visual observations in the EVCM images and

corroborate the reported "in vitro" findings between both staining protocols. Regarding PRO scoring or collagen fiber assessment, we saw no significant differences visible between different skin tones or the location of AKs when comparing FCF to acridine orange staining.

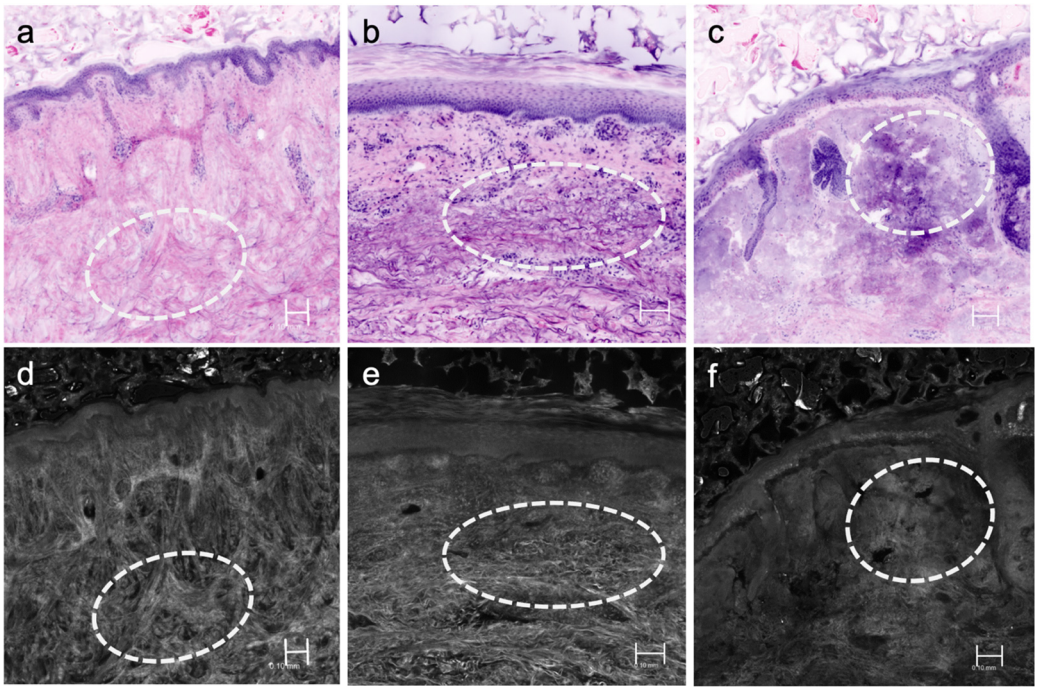

Figure 4. EVCM imaging of collagen fiber patterns in digital HE (**a**–**c**) and corresponding FCF fluorescence mode (**d**–**f**). White circles depict exemplarily regular collagen fibers (**a**,**d**) and altered collagen fibers with blurred lines (**b**,**e**), as well as damaged collagen fibers represented as degeneration patterns (**c**,**f**).

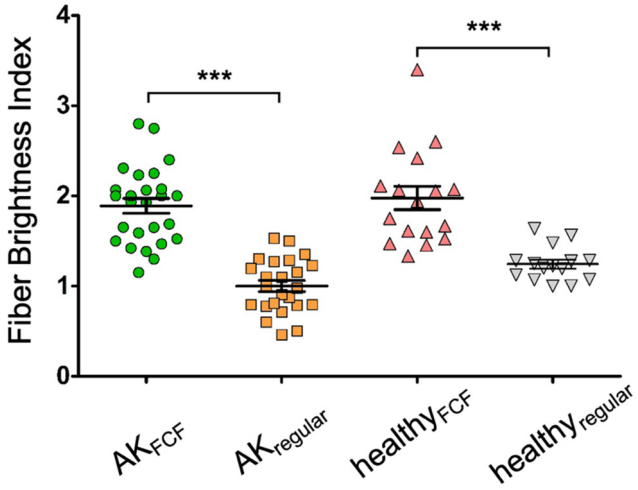

Figure 5. Scatter plot showing the quantitative results of the fiber brightness index (=FBI) in actinic keratoses (AK) and healthy skin imaged with the FCF and regular staining protocol. *** = $p < 0.001$.

4. Discussion

The accurate diagnosis and timely management of actinic keratoses (AKs) are essential to prevent their progression into invasive squamous cell carcinoma [34]. Since NMSC is frequently surrounded by UV-induced skin alterations like AKs, it is therefore important to evaluate the diagnostic workflow of these precancerous lesions for a simple and fast risk stratification. When the dermatologist/practitioner has no laboratory or pathologist

for cryosections nearby, EVCM may be a valid adjunction to fresh frozen sectioning or traditional histopathology. This imaging approach aligns with the growing interest in minimizing costly and time-consuming traditional histopathological procedures. Therefore, our study investigated the feasibility of PRO score assessment in EVCM images. EVCM therefore may provide dermatologists with a valuable tool to confidently diagnose and differentiate the stages of AKs in only a few minutes, providing a possibility for bedside assessment and prompt treatment initiation.

The use of a new staining protocol using FCF Fast Green furthermore proved to be a valid method for the visualization of UV-induced collagen alterations, offering the potential to assess the degree of collagen damage and its association with AK pathogenesis.

The observed disarray and fragmentation of collagen fibers within AK lesions are consistent with previous histopathological studies that have highlighted collagen remodeling as a hallmark of sun-induced skin damage [35–37]. These changes disrupt the skin's structural integrity, leading to functional changes, accompanied by an underlying inflammatory and oxidative response that affects the components of the extracellular matrix and triggers the activation of proteolytic enzymes such as metalloproteinases, potentially creating an environment conducive to the progression of precancerous lesions [38].

The quantitative analyses of collagen parameters confirmed our first visual impressions and revealed significant differences between AK lesions and healthy control skin. The decreased collagen density and altered orientation observed in AKs are consistent with the tissue remodeling characteristic of precancerous lesions. The increased collagen fragmentation further highlights the severity of collagen damage in these lesions. The early identification of precancerous lesions may therefore allow for proactive interventions and prevention of the progression to invasive malignancies. The ability of FCF Fast Green-enhanced EVCM to unveil collagen modifications that may, at an early stage, precede visible cellular atypia offers a unique advantage in enhancing the temporal resolution of diagnostics. These quantitative insights may contribute to more objective diagnostic criteria for AK assessment and potentially aid in risk stratification, reinforcing the diagnostic value of collagen imaging.

While in anhydrous conditions FCF Fast Green primarily targets collagen fibers, the capability of FGs binding affinity to collagen is significantly decreased in watery conditions. In this case, not only collagen but also elastic fibers are dyed. To maximize collagen affinity, our adjusted staining protocol included an additional step with rinsing in ethanol for 30 s for adequate tissue sample dehydration.

The choice of imaging dye is not a one-size-fits-all decision and depends on the specific formulation of the question. The further development of specific dyes may be advantageous in investigations targeting other molecular binding structures within the skin or assessing molecular interactions. However, they may fall short in studies necessitating a comprehensive view of cellular or collagen alterations without prior knowledge of specific targets. Conversely, FCF Fast Green's ease of application makes it particularly attractive for a broader range of applications and may facilitate its integration into routine clinical practice, where simplicity and efficiency are paramount. Future fields of investigation of FCF Fast Green-enhanced EVCM could be skin pathologies like the evolution of scar tissue, skin ageing, or connective tissue disorders/collagenopathies such as Ehlers–Danlos syndrome or osteogenesis imperfecta.

Although this study presents promising findings, several limitations warrant consideration. The relatively small sample size and single-center nature of the study may limit the generalizability of the results. Future directions for research could involve larger, multicenter studies to validate the diagnostic potential of FCF Fast Green-enhanced EVCM across diverse patient populations. Longitudinal studies tracking collagen alterations in AK lesions and assessing their predictive value for progression to invasive carcinoma could provide valuable insights into the clinical utility of this approach.

Moreover, during image acquisition, we also faced various technical obstacles. Due to fluctuations in the sample thickness, density, and quality, it was necessary to adjust the

applied pressure on the excised specimen as evenly as possible during tissue assembly. With regard to Pérez-Anker et al. [31,32], we therefore used a sponge specially tailored for this purpose and magnetic fixation of the sample on the object slide in order to achieve a straight tissue surface without air bubbles or wrinkles in the sample. In the rare case of remaining irregularities in the tissue surface due to, for example, contamination of the sample during the cutting process or too little ultrasound gel as a medium for the water immersion objective, serial recording at different penetration depths with subsequent fusion of the images reduced artifacts and enabled adequate image evaluation.

Concerning imaging with fluorescent dyes, it is also important to acknowledge that, during image acquisition, these dyes are irradiated with the excitation light, and the fluorophores are photochemically destroyed and lose their ability to fluoresce. The dynamics of this "photobleaching" depends on the intensity and energy of the excitation light on the one hand, and on the chemical composition of the fluorophores used on the other [39,40]. If there is a need for contiguous images of the same tissue, this bleaching effect has to be considered. When applying quantitative analyses like the calculation of the fiber brightness index, we therefore used representative keratinocyte nuclei as reference points, to compensate any differences in laser energy or dye concentration.

As the field of EVCM imaging continues to advance, future research directions should explore the development of novel dyes with enhanced properties, combining the target binding specificity with the accessibility and simplicity of stains like FCF Fast Green to pave the way for more precise diagnostics and personalized treatment strategies.

Regarding this topic, the field of EVCM imaging currently shows high inter-laboratory variability. Researchers across different laboratories and institutions often employ different equipment, dye concentrations, laser settings, and acquisition techniques, as well as diverse staining protocols, which can contribute to inconsistencies and variations in results that hinder direct comparisons between studies.

With a view to specific dyes, a multitude of different staining protocols and approaches with the absence of a standardized staining protocol poses significant challenges to consistency, reproducibility, and the translational potential of research findings. The establishment of standardized staining protocols could mitigate these challenges, advance EVCM imaging methodologies, and promote a more harmonized approach across laboratories to ensure that results obtained in one setting can be reliably extrapolated to others.

In the context of collaborative research, endeavors involving multiple centers and research groups are pivotal for large-scale studies and the generalizability of research outcomes. The absence of standardized staining protocols complicates multicenter collaborations, as variations in techniques may introduce confounding factors that are challenging to control. Standardization would also streamline collaborative efforts, enabling researchers to pool data with greater confidence and draw more meaningful conclusions from collective analyses.

5. Conclusions

In conclusion, our results highlight EVCM as a reliable tool for intraoperative AK PRO score assessment. The integration of FCF Fast Green demonstrated the diagnostic potential in identifying collagen alterations associated with actinic keratoses. By providing a clearer understanding of collagen changes within AKs, FCF Fast Green-enhanced EVCM offers a promising avenue for enhancing the accuracy of early solar elastosis and proactive clinical management.

The future standardization of staining protocols in EVCM imaging is not merely a procedural formality but a fundamental prerequisite for the advancement of the research field. By addressing multicenter collaborations, standardized protocols lay the groundwork for a more cohesive and impactful future in dermatological imaging research.

Author Contributions: Conceptualization, D.H. and M.D.; formal analysis, L.B. and M.D.; investigation, D.H., L.B., L.S. and M.D.; methodology, D.H., L.B. and M.D.; project administration, D.H. and L.E.F.; supervision, D.H., E.C.S. and L.E.F.; validation, D.H., L.B., L.S. and M.D.; writing—original

draft, L.B. and M.D.; writing—review and editing, D.H., E.C.S., L.E.F. and M.D. All authors have read and agreed to the published version of the manuscript.

Funding: This research received no external funding.

Institutional Review Board Statement: The study was conducted in accordance with the Declaration of Helsinki and approved by the local ethics committee of the LMU University Hospital (Ref.-Nr. 19-150).

Informed Consent Statement: Informed consent was obtained from all subjects involved in the study.

Data Availability Statement: The data presented in this study are available on request from the corresponding author.

Conflicts of Interest: The authors declare no conflicts of interest.

References

1. Hashim, P.W.; Chen, T.; Rigel, D.; Bhatia, N.; Kircik, L.H. Actinic Keratosis: Current Therapies and Insights into New Treatments. *J. Drugs Dermatol.* **2019**, *18*, s161–s166. [PubMed]
2. Eisen, D.B.; Asgari, M.M.; Bennett, D.D.; Connolly, S.M.; Dellavalle, R.P.; Freeman, E.E.; Goldenberg, G.; Leffell, D.J.; Peschin, S.; Sligh, J.E.; et al. Guidelines of care for the management of actinic keratosis. *J. Am. Acad. Dermatol.* **2021**, *85*, e209–e233. [CrossRef] [PubMed]
3. Reinehr, C.P.H.; Bakos, R.M. Actinic keratoses: Review of clinical, dermoscopic, and therapeutic aspects. *An. Bras. Dermatol.* **2019**, *94*, 637–657. [CrossRef] [PubMed]
4. Sterry, W.; Stockfleth, E. Maligne epitheliale Tumoren. In *Braun-Falco's Dermatologie, Venerologie und Allergologie*; Plewig, G., Ruzicka, T., Kaufmann, R., Hertl, M., Eds.; Springer: Berlin/Heidelberg, Germany, 2018; pp. 1801–1827. [CrossRef]
5. Christensen, R.E.; Elston, D.M.; Worley, B.; Dirr, M.A.; Anvery, N.; Kang, B.Y.; Bahrami, S.; Brodell, R.T.; Cerroni, L.; Elston, C.; et al. Dermatopathologic features of cutaneous squamous cell carcinoma and actinic keratosis: Consensus criteria and proposed reporting guidelines. *J. Am. Acad. Dermatol.* **2023**, *88*, 1317–1325. [CrossRef]
6. Cockerell, C.J. Histopathology of incipient intraepidermal squamous cell carcinoma ("actinic keratosis"). *J. Am. Acad. Dermatol.* **2000**, *42*, 11–17. [CrossRef]
7. Kesic, V.; Carcopino, X.; Preti, M.; Vieira-Baptista, P.; Bevilacqua, F.; Bornstein, J.; Chargari, C.; Cruickshank, M.; Erzeneoglu, E.; Gallio, N.; et al. The European Society of Gynaecological Oncology (ESGO), the International Society for the Study of Vulvovaginal Disease (ISSVD), the European College for the Study of Vulval Disease (ECSVD), and the European Federation for Colposcopy (EFC) consensus statement on the management of vaginal intraepithelial neoplasia. *Int. J. Gynecol. Cancer* **2023**, *33*, 446–461. [CrossRef]
8. Siddharthan, R.V.; Lanciault, C.; Tsikitis, V.L. Anal intraepithelial neoplasia: Diagnosis, screening, and treatment. *Ann. Gastroenterol.* **2019**, *32*, 257–263. [CrossRef]
9. Röwert-Huber, J.; Patel, M.J.; Forschner, T.; Ulrich, C.; Eberle, J.; Kerl, H.; Sterry, W.; Stockfleth, E. Actinic keratosis is an early in situ squamous cell carcinoma: A proposal for reclassification. *Br. J. Dermatol.* **2007**, *156* (Suppl. S3), 8–12. [CrossRef]
10. Fernandez-Figueras, M.T.; Carrato, C.; Saenz, X.; Puig, L.; Musulen, E.; Ferrandiz, C.; Ariza, A. Actinic keratosis with atypical basal cells (AK I) is the most common lesion associated with invasive squamous cell carcinoma of the skin. *J. Eur. Acad. Dermatol. Venereol.* **2015**, *29*, 991–997. [CrossRef]
11. Schmitz, L.; Gambichler, T.; Kost, C.; Gupta, G.; Stücker, M.; Stockfleth, E.; Dirschka, T. Cutaneous squamous cell carcinomas are associated with basal proliferating actinic keratoses. *Br. J. Dermatol.* **2019**, *180*, 916–921. [CrossRef]
12. Schmitz, L.; Gambichler, T.; Gupta, G.; Stücker, M.; Stockfleth, E.; Szeimies, R.M.; Dirschka, T. Actinic keratoses show variable histological basal growth patterns—A proposed classification adjustment. *J. Eur. Acad. Dermatol. Venereol.* **2018**, *32*, 745–751. [CrossRef] [PubMed]
13. Schmitz, L.; Kahl, P.; Majores, M.; Bierhoff, E.; Stockfleth, E.; Dirschka, T. Actinic keratosis: Correlation between clinical and histological classification systems. *J. Eur. Acad. Dermatol. Venereol.* **2016**, *30*, 1303–1307. [CrossRef] [PubMed]
14. Zalaudek, I.; Giacomel, J.; Argenziano, G.; Hofmann-Wellenhof, R.; Micantonio, T.; Di Stefani, A.; Oliviero, M.; Rabinovitz, H.; Soyer, H.P.; Peris, K. Dermoscopy of facial nonpigmented actinic keratosis. *Br. J. Dermatol.* **2006**, *155*, 951–956. [CrossRef] [PubMed]
15. Stadler, R.; Arheilger, B. Epidermale Tumoren. In *Histopathologie der Haut*; Cerroni, L., Garbe, C., Metze, D., Kutzner, H., Kerl, H., Eds.; Springer: Berlin/Heidelberg, Germany, 2016; pp. 557–597. [CrossRef]

16. Vladimirova, G.; Ruini, C.; Kapp, F.; Kendziora, B.; Ergün, E.Z.; Bağcı, I.S.; Krammer, S.; Jastaneyah, J.; Sattler, E.C.; Flaig, M.J.; et al. Ex vivo confocal laser scanning microscopy: A diagnostic technique for easy real-time evaluation of benign and malignant skin tumours. *J. Biophotonics* **2022**, *15*, e202100372. [CrossRef] [PubMed]
17. Longo, C.; Ragazzi, M.; Castagnetti, F.; Gardini, S.; Palmieri, T.; Lallas, A.; Moscarella, E.; Piana, S.; Pellacani, G.; Zalaudek, I.; et al. Inserting ex vivo fluorescence confocal microscopy perioperatively in Mohs micrographic surgery expedites bedside assessment of excision margins in recurrent basal cell carcinoma. *Dermatology* **2013**, *227*, 89–92. [CrossRef]
18. Longo, C.; Ragazzi, M.; Rajadhyaksha, M.; Nehal, K.; Bennassar, A.; Pellacani, G.; Malvehy Guilera, J. In Vivo and Ex Vivo Confocal Microscopy for Dermatologic and Mohs Surgeons. *Dermatol. Clin.* **2016**, *34*, 497–504. [CrossRef]
19. Hartmann, D. Ex vivo confocal laser scanning microscopy for melanocytic lesions and autoimmune diseases. *Hautarzt* **2021**, *72*, 1058–1065. [CrossRef]
20. Hartmann, D.; Ruini, C.; Mathemeier, L.; Bachmann, M.R.; Dietrich, A.; Ruzicka, T.; von Braunmuhl, T. Identification of ex-vivo confocal laser scanning microscopic features of melanocytic lesions and their histological correlates. *J. Biophotonics* **2017**, *10*, 128–142. [CrossRef]
21. Mentzel, J.; Stecher, M.M.; Paasch, U.; Simon, J.C.; Grunewald, S. Ex vivo confocal laser scanning microscopy with digital staining is able to map characteristic histopathological features and tissue reaction patterns of inflammatory skin diseases. *J. Eur. Acad. Dermatol. Venereol.* **2021**, *35*, e263–e265. [CrossRef] [PubMed]
22. Pérez-Anker, J.; Ribero, S.; Yélamos, O.; García-Herrera, A.; Alos, L.; Alejo, B.; Combalia, M.; Moreno-Ramírez, D.; Malvehy, J.; Puig, S. Basal cell carcinoma characterization using fusion ex vivo confocal microscopy: A promising change in conventional skin histopathology. *Br. J. Dermatol.* **2020**, *182*, 468–476. [CrossRef] [PubMed]
23. Shavlokhova, V.; Flechtenmacher, C.; Sandhu, S.; Pilz, M.; Vollmer, M.; Hoffmann, J.; Engel, M.; Freudlsperger, C. Detection of oral squamous cell carcinoma with ex vivo fluorescence confocal microscopy: Sensitivity and specificity compared to histopathology. *J. Biophotonics* **2020**, *13*, e202000100. [CrossRef] [PubMed]
24. Grupp, M.; Illes, M.; Mentzel, J.; Simon, J.C.; Paasch, U.; Grunewald, S. Routine application of ex vivo confocal laser scanning microscopy with digital staining for examination of surgical margins in basal cell carcinomas. *J. Dtsch. Dermatol. Ges.* **2021**, *19*, 685–692. [CrossRef] [PubMed]
25. Ulrich, M.; Lange-Asschenfeldt, S.; Gonzalez, S. Clinical applicability of in vivo reflectance confocal microscopy in dermatology. *G. Ital. Dermatol. Venereol.* **2012**, *147*, 171–178. [PubMed]
26. Al-Arashi, M.Y.; Salomatina, E.; Yaroslavsky, A.N. Multimodal confocal microscopy for diagnosing nonmelanoma skin cancers. *Lasers Surg. Med.* **2007**, *39*, 696–705. [CrossRef]
27. Cinotti, E.; Perrot, J.L.; Labeille, B.; Cambazard, F.; Rubegni, P. Ex vivo confocal microscopy: An emerging technique in dermatology. *Dermatol. Pract. Concept.* **2018**, *8*, 109–119. [CrossRef]
28. Segnani, C.; Ippolito, C.; Antonioli, L.; Pellegrini, C.; Blandizzi, C.; Dolfi, A.; Bernardini, N. Histochemical Detection of Collagen Fibers by Sirius Red/Fast Green Is More Sensitive than van Gieson or Sirius Red Alone in Normal and Inflamed Rat Colon. *PLoS ONE* **2015**, *10*, e0144630. [CrossRef] [PubMed]
29. López-De León, A.; Rojkind, M. A simple micromethod for collagen and total protein determination in formalin-fixed paraffin-embedded sections. *J. Histochem. Cytochem.* **1985**, *33*, 737–743. [CrossRef]
30. Timin, G.; Milinkovitch, M.C. High-resolution confocal and light-sheet imaging of collagen 3D network architecture in very large samples. *iScience* **2023**, *26*, 106452. [CrossRef]
31. Pérez-Anker, J.; Toll, A.; Puig, S.; Malvehy, J. Six steps to reach optimal scanning in ex vivo confocal microscopy. *J. Am. Acad. Dermatol.* **2022**, *86*, 188–189. [CrossRef]
32. Pérez-Anker, J.; Puig, S.; Malvehy, J. A fast and effective option for tissue flattening: Optimizing time and efficacy in ex vivo confocal microscopy. *J. Am. Acad. Dermatol.* **2020**, *82*, e157–e158. [CrossRef]
33. Schmitz, L.; Gupta, G.; Stücker, M.; Doerler, M.; Gambichler, T.; Welzel, J.; Szeimies, R.M.; Bierhoff, E.; Stockfleth, E.; Dirschka, T. Evaluation of two histological classifications for actinic keratoses—PRO classification scored highest inter-rater reliability. *J. Eur. Acad. Dermatol. Venereol.* **2019**, *33*, 1092–1097. [CrossRef]
34. Werner, R.N.; Stockfleth, E.; Connolly, S.M.; Correia, O.; Erdmann, R.; Foley, P.; Gupta, A.K.; Jacobs, A.; Kerl, H.; Lim, H.W.; et al. Evidence- and consensus-based (S3) Guidelines for the Treatment of Actinic Keratosis—International League of Dermatological Societies in cooperation with the European Dermatology Forum—Short version. *J. Eur. Acad. Dermatol. Venereol.* **2015**, *29*, 2069–2079. [CrossRef]
35. Rittié, L.; Fisher, G.J. Natural and sun-induced aging of human skin. *Cold Spring Harb. Perspect. Med.* **2015**, *5*, a015370. [CrossRef]
36. Fisher, G.J. The pathophysiology of photoaging of the skin. *Cutis* **2005**, *75*, 5–8; discussion 8–9. [PubMed]
37. Smith, J.G., Jr.; Davidson, E.A.; Sams, W.M., Jr.; Clark, R.D. Alterations in human dermal connective tissue with age and chronic sun damage. *J. Investig. Dermatol.* **1962**, *39*, 347–350. [CrossRef] [PubMed]
38. Schmitt, J.; Seidler, A.; Diepgen, T.L.; Bauer, A. Occupational ultraviolet light exposure increases the risk for the development of cutaneous squamous cell carcinoma: A systematic review and meta-analysis. *Br. J. Dermatol.* **2011**, *164*, 291–307. [CrossRef] [PubMed]

39. Karen, J.K.; Gareau, D.S.; Dusza, S.W.; Tudisco, M.; Rajadhyaksha, M.; Nehal, K.S. Detection of basal cell carcinomas in Mohs excisions with fluorescence confocal mosaicing microscopy. *Br. J. Dermatol.* **2009**, *160*, 1242–1250. [CrossRef] [PubMed]
40. Benson, D.M.; Bryan, J.; Plant, A.L.; Gotto, A.M., Jr.; Smith, L.C. Digital imaging fluorescence microscopy: Spatial heterogeneity of photobleaching rate constants in individual cells. *J. Cell Biol.* **1985**, *100*, 1309–1323. [CrossRef] [PubMed]